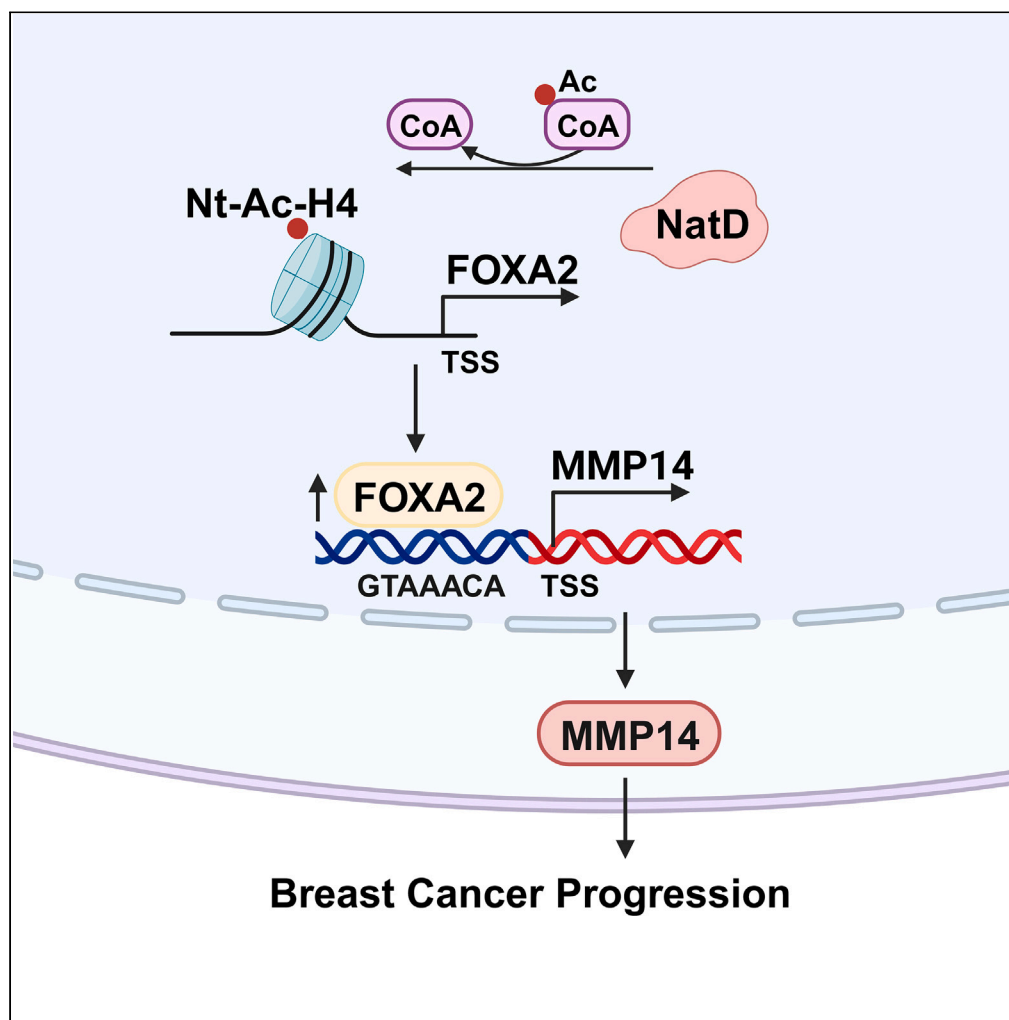


Article

NatD epigenetically activates FOXA2 expression to promote breast cancer progression by facilitating MMP14 expression



Mengying Xing,
Bing Yao, Jiakuan
Xu, ..., Jiwu Wei,
Lei Su, Quan Zhao

wjw@nju.edu.cn (J.W.)
suleinjingly@sina.com (L.S.)
qzhao@nju.edu.cn (Q.Z.)

Highlights

Upregulation of NatD is associated with poor prognosis in breast cancer patients

NatD promotes breast cancer cell migration and invasion *in vitro* and *in vivo*

NatD catalyzes the Nt-Ac-H4 of the FOXA2 promoter and promotes its expression

FOXA2 binds to the promoter of MMP14 and promotes its expression

Xing et al., iScience 27, 108840
February 16, 2024 © 2024 The
Author(s).
[https://doi.org/10.1016/
j.isci.2024.108840](https://doi.org/10.1016/j.isci.2024.108840)

Article

NatD epigenetically activates FOXA2 expression to promote breast cancer progression by facilitating MMP14 expression

Mengying Xing,¹ Bing Yao,² Jiakuan Xu,¹ Peifen Lu,¹ Qixiang Li,¹ Dongliang Wu,¹ Bing Chen,¹ Jiwu Wei,^{3,*} Lei Su,^{1,*} and Quan Zhao^{1,4,*}

SUMMARY

N- α -acetyltransferase D (NatD) mediates N- α -terminal acetylation of histone H4 (Nt-Ac-H4), but its role in breast cancer metastasis remains unknown. Here, we show that depletion of NatD directly represses the expression of FOXA2, and is accompanied by a significant reduction in Nt-Ac-H4 enrichment at the FOXA2 promoter. We show that NatD is commonly upregulated in primary breast cancer tissues, where its expression level correlates with FOXA2 expression, enhanced invasiveness, and poor clinical outcomes. Furthermore, we show that FOXA2 promotes the migration and invasion of breast cancer cells by activating MMP14 expression. MMP14 is also upregulated in breast cancer tissues, where its expression level correlates with FOXA2 expression and poor clinical prognosis. Our study shows that the NatD-FOXA2-MMP14 axis functions as a key signaling pathway to promote the migratory and invasive capabilities of breast cancer cells, suggesting that NatD is a critical epigenetic modulator of cell invasion during breast cancer progression.

INTRODUCTION

N- α -terminal acetylation (Nt-Ac) is a ubiquitous protein modification that occurs on 80%–90% of human proteins.¹ Nt-Ac is essential for various biological functions, including protein-protein interactions, protein complex formation, cellular apoptosis, rDNA transcriptional regulation, cellular metabolism, protein subcellular localization, and protein degradation.^{2–5} Nt-Ac modification is catalyzed by N-terminal acetyltransferases (NATs), which serve to transfer the acetyl group from acetyl-coenzyme A (Ac-CoA) to the N- α -terminal amino group of the protein substrates.⁶ In humans, there are seven evolutionarily conserved NATs, NatA–NatF and NatH, which are composed of catalytic and potentially auxiliary subunits.⁷ NatD (also known as NAA40, NAT11, or Patt1) activity was first observed in the yeast *Saccharomyces cerevisiae*, which mediates the Nt-acetylation of histone H4 and H2A exclusively.⁸

The involvement of NATs in cell fate and cancers is being increasingly recognized. NatD-catalyzed Nt-Ac not only has various effects on protein function but also regulates the establishment and crosstalk of histone modifications that impact both chromatin structure and gene expression.^{9–11} We previously showed that Nt-Ac-H4 suppresses Ser1 phosphorylation of histone H4 and induces Slug transcription to promote epithelial-to-mesenchymal transition (EMT) in lung cancer.⁹ NatD is downregulated in hepatocellular carcinoma, and the overexpression of NatD in cancerous cells enhances apoptosis.¹² The knockout of NatD induces p53-independent apoptosis through the mitochondrial pathway in colorectal cancer (CRC) cells.¹³ In addition, NatD promotes the growth of CRC cells by promoting oncogene expression through the upregulation of protein arginine methyltransferase 5 (PRMT5).¹⁰ Based on these cancer-related studies, NatD plays an important role in tumorigenesis. However, the role of NatD in breast cancer remains largely unknown.

In the present study, we investigated the effect of NatD on breast cancer progression. We found that NatD knockdown suppressed the migration and invasion of breast cancer cells. Mechanistically, we identified forkhead box protein A2 (FOXA2) as a key downstream target gene of NatD, which directly regulates the transcriptional expression of matrix metalloproteinase 14 (MMP14). FOXA2, also known as hepatocyte nuclear factor 3- β , is a member of the forkhead box class of DNA-binding proteins.^{14,15} Various members of the FOX transcription factor family are widely distributed in eukaryotes and contain a forkhead domain (also known as the winged-helix domain) flanked by sequences required for nuclear localization.^{16–18} FOXA2 is a key regulator in the formation of node-, notochord-, nervous system-, and endoderm-derived structures.^{19,20} Importantly, FOXA2 plays a significant role in the progression of multiple cancers, including colon cancer, ovarian cancer, and liver cancer.^{21–23} MMP14 is a member of the membrane-type matrix metalloproteases, which are pivotal regulators of

¹The State Key Laboratory of Pharmaceutical Biotechnology, Department of Hematology and General Surgery, The Affiliated Drum Tower Hospital of Nanjing University Medical School, China-Australia Institute of Translational Medicine, School of Life Sciences, Nanjing University, Nanjing 210046, China

²National Experimental Teaching Center of Basic Medical Science, Nanjing Medical University, Nanjing, China

³Jiangsu Key Laboratory of Molecular Medicine, Medical School of Nanjing University, Nanjing, China

⁴Lead contact

*Correspondence: wjw@nju.edu.cn (J.W.), suleinjg@nju.edu.cn (L.S.), qzhao@nju.edu.cn (Q.Z.)

<https://doi.org/10.1016/j.isci.2024.108840>



cell invasion, growth, and survival. MMPs are involved in the breakdown of extracellular matrix in embryonic development, reproduction, arthritis, and tumor metastasis.^{24–27} MMP14 can activate MMP2 protein, and this activity is associated with tumor invasion.^{28,29} We show that the NatD-FOXA2-MMP14 axis modulates the progression of breast cancer, suggesting that NatD may be a potential therapeutic target for breast cancer.

RESULTS

Upregulation of NatD is correlated with lymph node metastasis and poor prognosis of patients with breast cancer

To investigate the clinical relevance of NatD expression in breast cancer, we first examined NatD expression in breast cancer specimens from a cohort of 132 patients by immunohistochemistry using specific anti-NatD and Nt-Ac-H4 antibodies. Significantly higher expression levels of NatD and Nt-Ac-H4 staining were observed in breast cancer tissues than in matched adjacent normal tissues from patients (Figures 1A and 1B). In addition, we analyzed the correlation between NatD expression and clinicopathological characteristics in patients with breast cancer. Notably, we found that NatD expression was positively correlated with higher grade lymph node status (Figure 1C; Tables S1 and S2). Importantly, we found that poor prognosis was correlated with higher expression of NatD in breast cancer (Figure 1D). We further compared the protein expression levels of NatD from tissues of different subtypes, including luminal, HER2-positive, and triple-negative breast cancer, but obtained no consistent differences (Figure 1E). We later retrieved data from the TCGA and CPTAC databases and confirmed that the mRNA and protein expression levels of NatD were significantly higher in breast cancer tissues than in adjacent normal tissues (Figures 1F and 1H) and independent of breast cancer subtype (Figures 1G and 1I). These results indicated that the higher the NatD expression was in breast cancer, the higher the malignant degree and the worse the prognosis despite the presence of different breast cancer subtypes.

NatD promotes breast cancer cell migration and invasion

To examine the role of NatD in breast cancer cell-invasive capability, we used the CRISPR-Cas9 system to knock out NatD in two breast cancer cell lines, MDA-MB-231 and MCF7. We confirmed successful depletion of NatD (NatD-KO) in both cell lines by western blot analysis and genomic DNA sequencing (Figures 2A, 2B, and S1A). Later, transwell assays were applied to assess the effects of NatD on cell migration and invasion of breast cancer cells *in vitro*. We found that NatD depletion significantly reduced the migratory and invasive capabilities of MDA-MB-231 or MCF7 cells compared to wild-type (WT) control cells (Figures 2E, 2G, S1B, and S1F). In addition, we overexpressed NatD in MDA-MB-231 or MCF7 cells. Overexpression of NatD was confirmed by western blot analysis (Figures 2C and 2D). Results from transwell assays showed that NatD overexpression (NatD-OE) significantly enhanced the migration and invasion of MDA-MB-231 or MCF7 cells compared to empty vector control cells (Figures 2F, 2H, S1C, and S1G). To determine whether the regulation of migration and invasion by NatD was acetyltransferase activity dependent in breast cancer cells, we constructed a mutant plasmid of NatD (NatD Δ) in which four amino acids (RRKG, aa147–150) located in the Ac-CoA-binding motif were deleted (Figure S1D).⁹ As shown in Figure 2I, we detected significantly reduced expression levels of Nt-Ac-H4 in NatD Δ cells compared with the wild-type NatD cells by western blot analysis. Furthermore, transwell assay showed that cell migratory and invasive capabilities of breast cancer cells were significantly reduced in NatD Δ cells compared with the wild-type NatD cells (Figures 2J and S1E). In order to further examine the metastatic role of NatD *in vivo*, NatD-depleted MDA-MB-231-luc cells were injected into the tail veins of nude mice. Through live-imaging monitoring, we found that the depletion of NatD significantly reduced the formation of metastatic foci in the lungs of mice compared to WT control mice (Figures 2K–2M). H&E and immunohistochemistry (IHC) staining further verified that NatD knockout significantly reduced Nt-Ac-H4 levels in lung metastatic foci compared to WT control tissues (Figure 2N). These results indicate that NatD promotes breast cancer cell migration and invasion *in vivo*.

NatD directly activates the expression of FOXA2 in breast cancer cells

To investigate the molecular mechanism by which NatD promotes breast cancer cell migration and invasion, we performed RNA sequencing analysis using NatD-depleted MDA-MB-231 cells and wild-type control cells. We identified 119 upregulated and 216 downregulated mRNAs ($|\log_2\text{Ratio}| \geq 1$ and q value ≤ 0.05) in NatD knockout cells compared to wild-type control cells (Figure 3A, GEO database under accession number GSE230625). The effect of NatD knockout on gene-function categories was analyzed by gene ontology (GO) enrichment analysis. Positive regulation of cell adhesion and migration was among the top five significantly differentially expressed categories of genes related to biological function (Figure 3B). Gene set enrichment analysis indicated that NatD knockout differentially affected the expression of genes associated with metastasis (Figure 3C). Collectively, these results indicate that NatD function is tightly associated with cell adhesion and migration in breast cancer cells. Subsequently, we performed a heatmap analysis of differentially expressed genes related to cell adhesion and migration. On the heatmap, we found 10 key differentially expressed genes, including FOXA2, ADAMTS1, CD44, CXCR4, ITGB2, ITGB3, MMP1, MMP14, MMP9, and E-cadherin, that play key roles in cell adhesion and migration and are involved in metastasis,^{30–34} and which were significantly downregulated when NatD was knocked out (Figure S2A). We analyzed and rechecked the expression of these genes and found that FOXA2 was the most downregulated gene in MDA-MB-231 knockout cells compared to wild-type cells (Figure 3D). Western blot assays verified that the protein levels of FOXA2 were significantly downregulated in NatD-depleted MDA-MB-231 cells compared to wild-type control cells (Figure 3E). We also obtained consistent results from NatD-knockout MCF7 cells (Figures 3F and 3G). In line with these results, chromatin immunoprecipitation (ChIP) analysis with Nt-Ac-H4 antibody showed that Nt-Ac-H4 enrichment on the FOXA2 promoter was greatly reduced in NatD knockout cells compared to wild-type cells (Figure 3H). To assess the clinical relevance of FOXA2 expression in patients with breast cancer, we examined FOXA2 expression in breast cancer tissue specimens by immunohistochemistry using a specific anti-FOXA2 antibody. IHC staining analysis

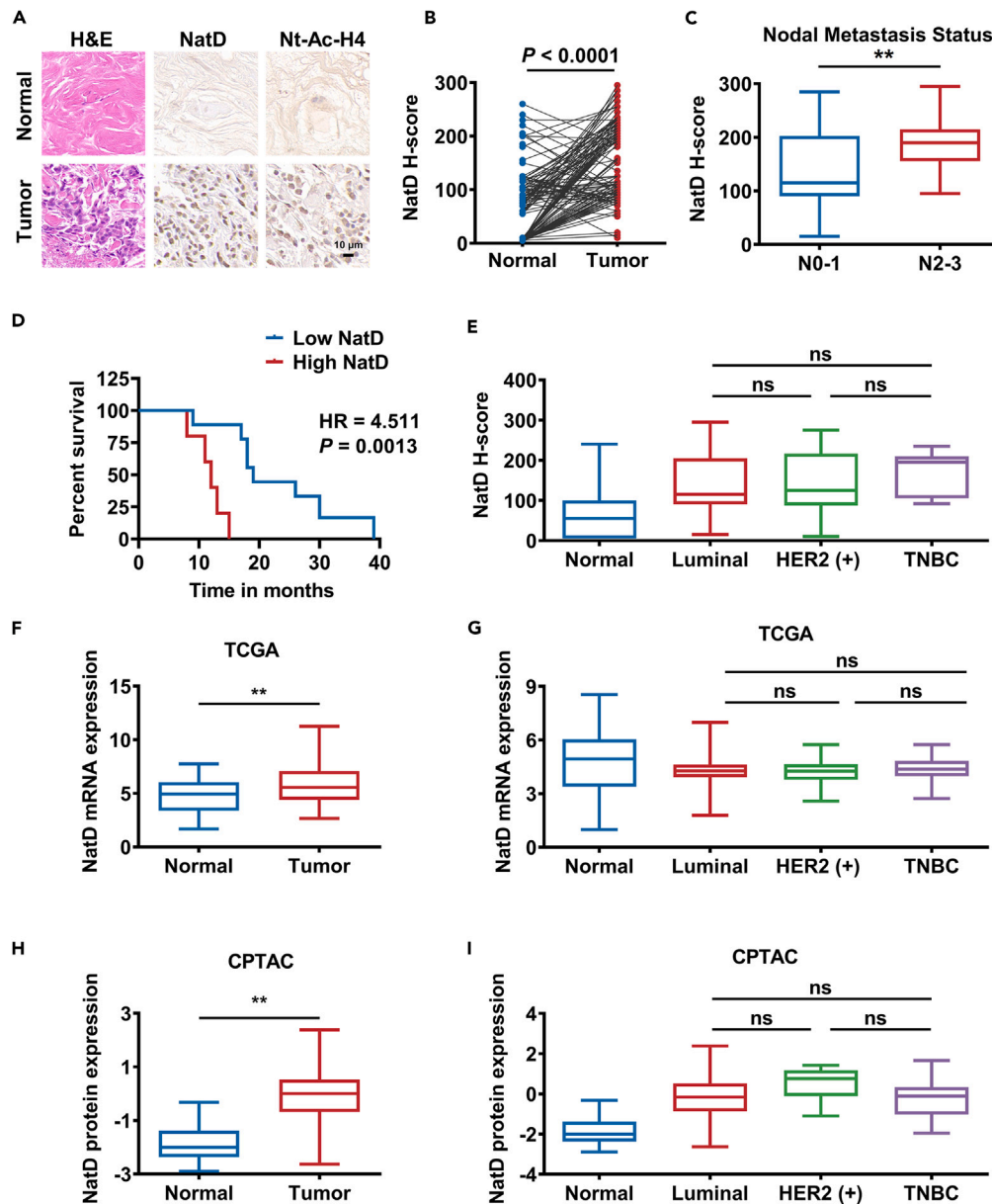


Figure 1. Upregulation of NatD is correlated with lymph node metastasis and poor prognosis of patients with breast cancer

(A) Representative images of H&E staining and IHC staining of NatD and Nt-Ac-H4 in matched normal and breast cancer tissues. Scale bar, 10 μ m.

(B) Total IHC score of NatD in matched normal and breast cancer tissues. $n = 132$ pairs of tissue samples; Student's t test, $p < 0.0001$.

(C) Correlation between NatD expression and lymph node metastasis in breast cancer patients. Student's t test, $n(N0-1) = 89$, $n(N2-3) = 21$, $**p < 0.01$. Data are represented as mean \pm SD.

(D) Kaplan-Meier plots of overall survival of patients with breast cancer stratified by NatD expression. Log rank test, $n = 14$, $p = 0.0013$, hazard ratio (HR) = 4.511.

(E) The IHC score of NatD in luminal ($n = 99$), HER2-positive ($n = 26$), and TNBC ($n = 7$) breast cancer and normal tissues ($n = 132$). One-way ANOVA test; ns, not significant. Data are represented as mean \pm SD.

(F) The mRNA expression of NatD in breast cancer ($n = 1109$) and normal ($n = 113$) tissues was analyzed from TCGA data. Student's t test, $**p < 0.01$. Data are represented as mean \pm SD.

(G) The mRNA expression of NatD in luminal ($n = 707$), HER2-positive ($n = 68$), and TNBC ($n = 115$) breast cancer and normal tissues ($n = 113$) was analyzed from TCGA data. One-way ANOVA test; ns, not significant. Data are represented as mean \pm SD.

(H) The protein expression of NatD in breast cancer ($n = 125$) and normal ($n = 18$) tissues was analyzed from the CPTAC data. Student's t test, $**p < 0.01$. Data are represented as mean \pm SD.

(I) The protein expression of NatD in luminal ($n = 64$), HER2-positive ($n = 10$), and TNBC ($n = 16$) breast cancer and normal tissues ($n = 18$) was analyzed from the CPTAC data. One-way ANOVA test; ns, not significant. Data are represented as mean \pm SD.

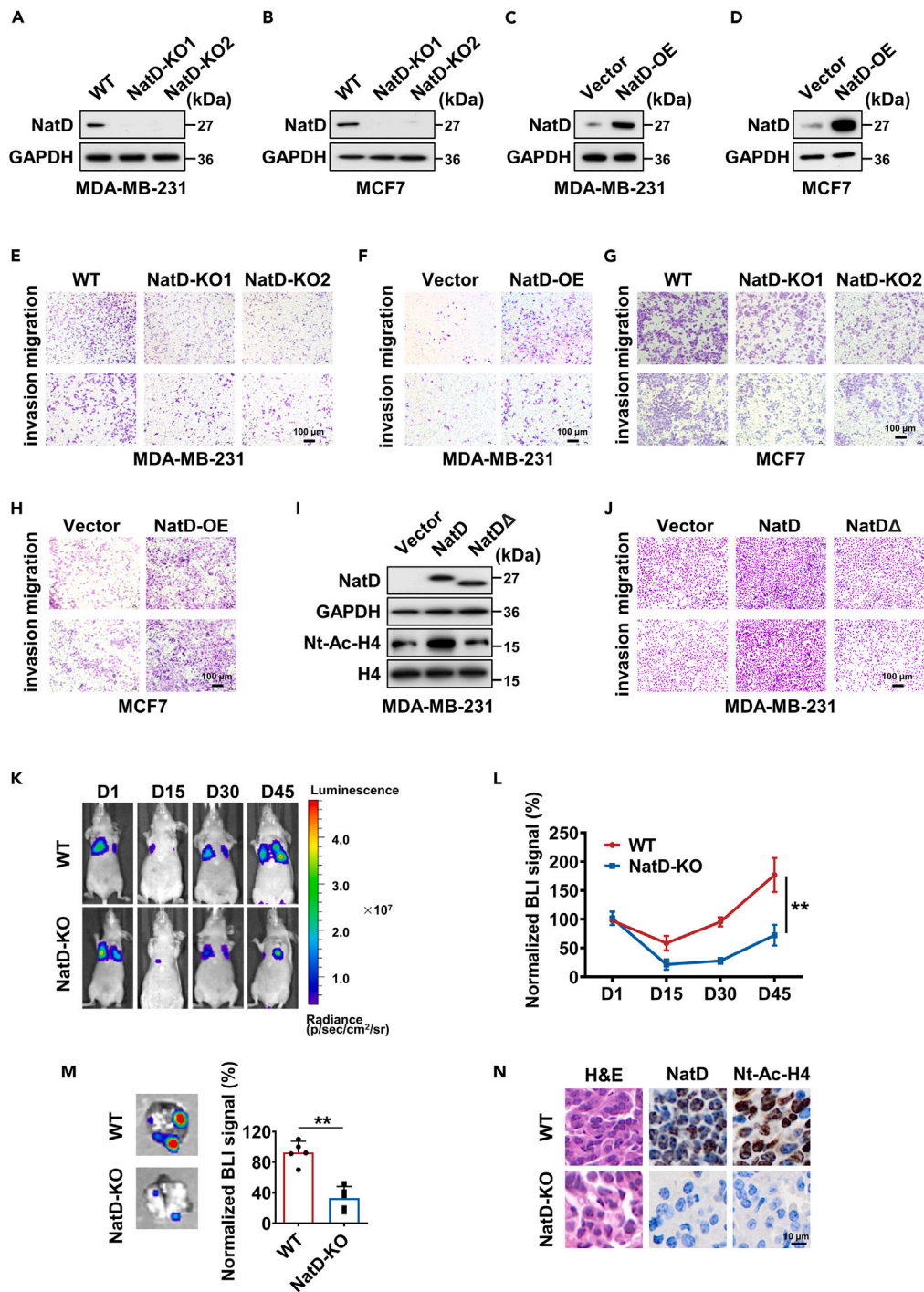


Figure 2. NatD promotes breast cancer cell migration and invasion

(A and B) Protein levels of NatD in wild-type (WT) and NatD knockout (NatD-KO) MDA-MB-231 (A) and MCF7 (B) cells were detected by western blot analysis. GAPDH was used as an internal control.

(C and D) Protein levels of NatD in vector control and NatD-overexpressing (NatD-OE) MDA-MB-231 (C) and MCF7 (D) cells were detected by western blot analysis.

(E and F) The effect of NatD knockout (E) or overexpression (F) on the migration and invasion of MDA-MB-231 cells was assessed by Transwell assays. Scale bar, 100 μ m.

(G and H) Cell migration and invasion were assessed by Transwell assays in NatD-KO (G) or NatD-OE (H) MCF7 cells. Scale bar, 100 μ m.

Figure 2. Continued

- (I) Protein levels of NatD and Nt-Ac-H4 in MDA-MB-231 cells transfected with wild-type NatD or NatD Δ expression plasmid. GAPDH and histone H4 served as internal control.
- (J) The migration and invasion of MDA-MB-231 cells transfected with wild-type NatD or NatD Δ expression plasmid were assessed by Transwell assays. Scale bar, 100 μ m.
- (K) Representative bioluminescent (BLI) images acquired at the indicated time points after intravenous injection of nude mice with WT and NatD-KO MDA-MB-231-luc cells from day 1 (D1) to day 45 (D45). Pseudocolor heatmaps indicate the intensity of bioluminescence from low (blue) to high (red).
- (L) Normalized BLI signals of lung tumors of corresponding mice recorded at the indicated time points. Two-way ANOVA test, $n = 5$, ** $p < 0.01$. Data are represented as mean \pm SD.
- (M) (left) Representative images showing luciferase activity in lungs from nude mice acquired 45 days after intravenous injection with WT or NatD-KO MDA-MB-231-luc cells. (right) Quantification of total lung bioluminescence from nude mice in the WT and NatD-KO groups. Student's t test, $n = 5$, ** $p < 0.01$. Data are represented as mean \pm SD.
- (N) Representative images of H&E- and IHC-stained histological sections of lungs from nude mice injected with WT and NatD-KO MDA-MB-231-luc cells. Scale bar, 10 μ m.

showed that FOXA2 was mainly localized to the nucleus, and its expression levels were markedly increased in breast cancer tissues compared to adjacent normal tissues (Figure 3I). Importantly, Kaplan-Meier survival analysis showed that breast cancer patients with high FOXA2 expression had shorter overall survival ($p = 0.0015$, Figure 3J) and the overall survival prognosis was poorer in the high NatD + high FOXA2 expression group compared with that in the low NatD + low FOXA2 group ($p = 0.0037$, Figure S2B). As well, Kaplan-Meier survival analysis showed shorter recurrence-free survival in breast cancer patients with high FOXA2 expression (Figure S2C). Notably, the expression of FOXA2 was positively correlated with higher grade lymph node status (Figure 3K). And the expression of NatD was positively correlated with the expression of FOXA2 in human breast cancer tissues (Figure 3L). Intriguingly, it was consistent with the results that we analyzed using the public GEO database (GSE12093, Figure S2D). These results indicated that NatD directly activates the expression of FOXA2 in breast cancer cells.

FOXA2 is involved in NatD-promoted breast cancer cell migration and invasion

Given that FOXA2 is a key direct downstream target of NatD in breast cancer cells, we tested whether FOXA2 is critical for NatD-promoted breast cancer cell invasion. We found that NatD knockout significantly reduced the migratory and invasive capabilities of MDA-MB-231 cells compared to wild-type control cells (Figures 4A, 4B, and S2E). Of importance, the migratory and invasive phenotypes could be reversed by enforced overexpression of FOXA2 in NatD knockout cells (Figures 4A, 4B, and S2E). Similar rescue results were obtained with MCF7 cells (Figures 4C, 4D, and S2F). We then examined the role of FOXA2 *in vivo*. In agreement with the *in vitro* results, we found that the restoration of FOXA2 could significantly reverse the reduction in lung metastasis in NatD knockout MDA-MB-231 tumors (Figures 4E–4G). Results from H&E and IHC staining verified NatD and FOXA2 expression and showed that NatD knockout was accompanied by a reduced level of Nt-Ac-H4 (Figure 4H). These results further indicated that FOXA2 plays a key role in NatD-promoted breast cancer cell invasion *in vivo*.

MMP14 is a direct downstream target of FOXA2 in breast cancer cells

Previously, GO enrichment analysis revealed that matrisome-associated genes, which include extracellular matrix regulators such as MMPs and ADAMs,³⁵ were the top differentially expressed category of genes when NatD was knocked out in MDA-MB-231 cells (Figure 3B). In fact, we have shown that NatD regulates a spectrum of genes in breast cancer cells, including three matrix metalloproteinases, MMP1, MMP9, and MMP14 (Figures 3D and S2A). FOXA2, as a transcription factor, has been previously reported to be related to the transcription of MMP9 and MMP12.^{36,37} Interestingly, after examining the promoters of MMP1, MMP9, and MMP14, we found FOXA2-binding sites at the proximal promoter regions of these MMP genes (<https://jaspar.genereg.net>, Figure 5A). To determine whether these MMPs were involved in the tumor-promoting role of FOXA2 in breast cancer cells, mRNA expression of MMPs was examined by quantitative reverse transcription PCR analysis in MDA-MB-231 cells with FOXA2 knockdown. We found that reduction of MMP14 expression in FOXA2 knockdown MDA-MB-231 cells was significantly greater than the reduction of MMP1 and MMP9 (Figure 5B). We found that both MMP14 mRNA and protein levels were significantly downregulated in FOXA2 knockdown MDA-MB-231 or MCF7 cells compared to scrambled negative control (NC) siRNA-treated cells (Figures 5B–5E). Conversely, we found that both MMP14 mRNA and protein were significantly upregulated in FOXA2-overexpressing MDA-MB-231 or MCF7 cells compared to vector control cells (Figures 5F–5I). Results of ChIP analysis showed that the enrichment of FOXA2 was significantly reduced in FOXA2 knockdown cells at the MMP14 promoter compared to NC control cells (Figure 5J). Consistent with this finding, ChIP analysis showed that the enrichment of FOXA2 was significantly increased at the MMP14 promoter in FOXA2-OE MDA-MB-231 cells compared to vector control cells (Figure 5K). As shown in Figures 5L and 5O, the protein expression of MMP14 was decreased upon NatD knockdown, while the protein levels were rescued after FOXA2 overexpression in NatD knockdown breast cancer cells. Functionally, we found that restoration of MMP14 could significantly reverse the phenotypic changes in MDA-MB-231 or MCF7 breast cancer cells induced by FOXA2 knockdown (Figures 5M, 5N, 5P, 5Q, S2G, and S2H). These results suggest that MMP14 is a direct downstream target of FOXA2 and promotes breast cell migration and invasion.

Upregulation of MMP14 is associated with poor prognosis in breast cancer patients

To further investigate the clinical relevance of MMP14 expression in breast cancer, we examined MMP14 expression in breast cancer tissue specimens by immunohistochemistry using a specific anti-MMP14 antibody. H&E and IHC staining revealed that the protein level of

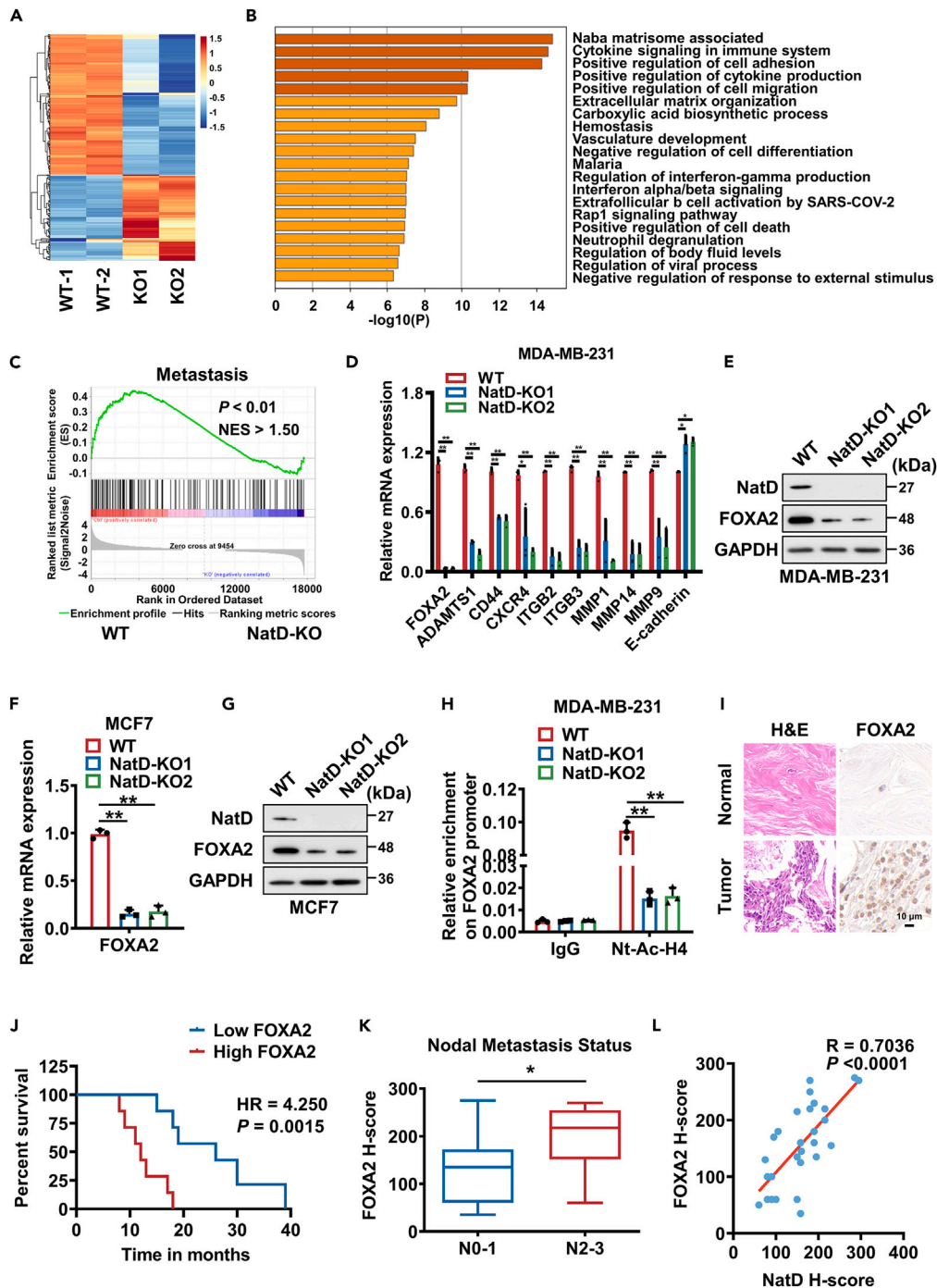


Figure 3. NatD directly activates the expression of FOXA2 in breast cancer cells

(A) Heatmaps from RNA-seq data (GEO database under accession number GSE230625) showing overlapping differentially expressed genes (DEGs) in WT and NatD-KO MDA-MB-231 cells.

(B) Gene ontology (GO) analysis identified the top 20 most significant GO terms.

(C) Gene set enrichment analysis (GSEA) indicated that the identified differentially expressed genes were enriched for metastasis-associated genes. $p < 0.01$, NES > 1.50 .

(D) The mRNA expression of DEGs was measured by qRT-PCR in WT and NatD-KO MDA-MB-231 cells. One-way ANOVA test, $n = 3$, * $p < 0.05$, ** $p < 0.01$ vs. indicated control. Data are represented as mean \pm SD.

(E) Western blot of the indicated proteins in WT and NatD-KO MDA-MB-231 cells.

Figure 3. Continued

(F and G) The mRNA (F) and protein (G) expression of FOXA2 were measured by qRT-PCR and western blot analysis in WT and NatD-KO MCF7 cells. One-way ANOVA test, $n = 3$, $**p < 0.01$ vs. indicated control. Data are represented as mean \pm SD.

(H) ChIP analysis of Nt-Ac-H4 enrichment on the promoter region of the FOXA2 gene in MDA-MB-231 cells. One-way ANOVA test, $n = 3$, $**p < 0.01$ vs. indicated control. Data are represented as mean \pm SD.

(I) Representative images of H&E staining and IHC staining of FOXA2 in matched normal and breast cancer tissues. Scale bar, 10 μ m.

(J) Kaplan-Meier plots of overall survival of patients with breast cancer stratified by FOXA2 expression. Log rank test, $n = 14$, $p = 0.0015$, HR = 4.250.

(K) Correlation between FOXA2 expression and lymph node metastasis in breast cancer patients. Student's t test, $n(N0-1) = 18$, $n(N2-3) = 10$, $*p < 0.05$. Data are represented as mean \pm SD.

(L) The correlation analysis of NatD and FOXA2 levels in breast cancer tissues. Pearson correlation, $n = 28$, $R = 0.7036$, $p < 0.0001$.

MMP14 was significantly upregulated in breast cancer tissues compared to normal tissues (Figure 6A). We also retrieved data from the UALCAN website and found that MMP14 mRNA expression was remarkably higher in breast cancer tissues than in normal tissues (Figure S3A). Importantly, Kaplan-Meier survival analysis showed that breast cancer patients with higher MMP14 expression had shorter overall survival ($p = 0.0043$, Figure 6B). The overall survival prognosis was poorer in the high NatD + high MMP14 expression group compared with that in the low NatD + low MMP14 group ($p = 0.0051$, Figure S3B). The overall survival prognosis was poorer in the high FOXA2 + high MMP14 expression group compared with that in the low FOXA2 + low MMP14 group ($p = 0.0139$, Figure S3C). Similarly, Kaplan-Meier survival analysis showed that breast cancer patients with high MMP14 expression had shorter relapse-free survival (Figure S3D). Notably, we found that MMP14 expression positively correlated with higher grade lymph node status (Figure 6C), this is consistent with the results that we analyzed using the public GEO database (GSE9893, Figure S3E). In addition, MMP14 expression levels positively correlated with NatD or FOXA2 expression levels in human breast cancer tissues (Figures 6D and 6E), this is consistent with the results that we analyzed using the public GEO database (GSE12093, Figure S3F). Collectively, these data suggest that upregulation of MMP14 is associated with poor prognosis in breast cancer patients.

DISCUSSION

Increased knowledge regarding NAT biology and structure acquired over the past decade has led to their recognition as potential therapeutic targets for cancer treatment.³⁸ In this study, we show that NatD, which mediates N- α -terminal acetylation of histone H4, is upregulated in breast cancer and promotes the migratory and invasive capabilities of breast cancer cells *in vitro* and *in vivo*, suggesting a potentially novel therapeutic target for breast cancer metastasis.

Recent findings have implicated deregulation of the evolutionarily conserved NatD enzyme toward Nt-Ac on histone H4 in different types of cancer, such as liver, lung, and CRC.^{9,39,40} Zhen et al. reported that NatD is highly expressed in the liver, is downregulated in hepatocellular carcinoma (HCC), and promotes apoptosis of HCC cells.¹² However, in contrast to this report, Koufaris et al. recently discovered that NatD was associated with the cell cycle, DNA replication, and RNA transport and that increased NatD expression correlated with decreased patient survival supporting a novel carcinogenic effect in liver cancer.^{11,41} We have previously reported that NatD is highly expressed in lung cancer and promotes the migration and invasion of lung cancer cells.⁹ Demetriadou et al. revealed that NatD depletion and subsequent repression of PRMT5 results in altered expression of key oncogenes and tumor suppressor genes, leading to inhibition of CRC growth.¹⁰ We show here that the NatD-FOXA2-MMP14 axis functions as a key signaling pathway to promote migratory and invasive capabilities of breast cancer cells regardless of tumor molecular subtypes, providing another example in which NAT participates in tumor progression modulation (Figure 6F). Recently, some inhibitors have been reported for this important acetyltransferase.^{42,43} Given that NatD promotes breast cancer cell metastasis, NatD enzymatic inhibition may provide an epigenetic therapeutic strategy for breast cancer. In the current study, we show that FOXA2 acts as a key factor mediating the function of NatD and MMP14 in breast cancer cells. FOXA2, a member of the FOXA family of the forkhead box transcription factors, has been implicated as a potential marker for diverse cancers.^{14,21,44} FOXA2 can promote EMT, inhibit apoptosis, and enhance the invasive ability of colon cancer cells by upregulating vimentin and downregulating E-cadherin expression.²¹ FOXA2 can also promote the migration and metastasis of esophageal cancer by activating CXCR4 expression.³² Thus, we speculate that NatD may be crucial for breast cancer metastasis by acting as a modulator of the transcription factor FOXA2. However, in contrast to these reports, Christina et al. revealed that deletion of FOXA2 leads to upregulation of the PLAU and ERK signaling pathways, which promotes the growth of pancreatic cancer.⁴⁵ FOXA2 can bind to the CDH1 promoter, enhance the expression of its gene product, E-cadherin, and reduce oral cancer cell migration.⁴⁶ These findings imply that FOXA2 can act as either an oncogene or a tumor suppressor in a context-dependent manner, which deserves further characterization in the future.

During metastasis, carcinoma cells acquire the ability to invade surrounding tissues and intravasate through the endothelium to enter systemic circulation.³³ The events leading to metastasis are often similar in different types of solid tumors and rely heavily on the proteolytic activity of numerous MMPs, which affect tissue integrity, immune cell recruitment, and tissue turnover by degrading the extracellular matrix components and by releasing matrikines, cell surface-bound cytokines, growth factors, or their receptors.^{47,48} MMP14 was one of the first reported membrane-type MMPs.³⁴ Among the MMPs, MMP14 is the driving force behind extracellular matrix and tissue destruction during cancer invasion and metastasis. MMP14 also influences both intercellular and cell-matrix communication by regulating the activity of many membrane-anchored plasmas and extracellular proteins.²⁴ Moreover, MMP14 plays a role in various biological processes in both normal and cancerous tissues.⁴⁹ MMP14 is essential for normal development, and loss of MMP14 in mice leads to increased perinatal mortality and causes cell senescence and nuclear defects.^{50,51} In human endothelial cells, downregulation of MMP14 inhibits angiogenesis.⁵² As the master MMP, MMP14 is

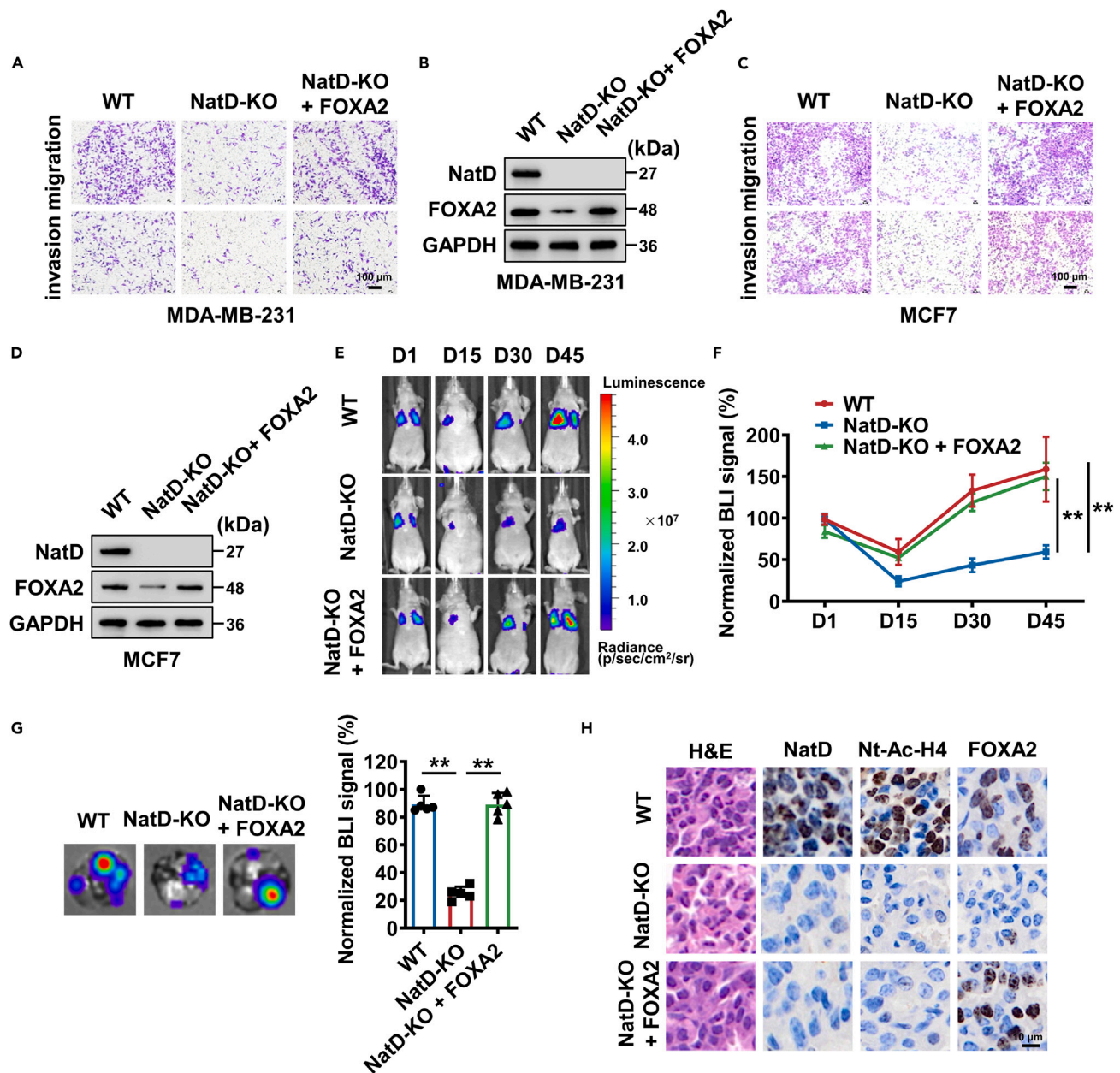


Figure 4. FOXA2 is involved in NatD-promoted breast cancer cell migration and invasion

(A and C) Transwell assays of MDA-MB-231 (A) and MCF7 (C) cells with WT, NatD-KO, or NatD-KO + FOXA2. Scale bar, 100 μ m.

(B and D) Protein levels of NatD and FOXA2 in MDA-MB-231 (B) and MCF7 (D) cells with WT, NatD-KO, or NatD-KO + FOXA2 were detected by western blot analysis. GAPDH was used as an internal control.

(E) Representative bioluminescent (BLI) images acquired at the indicated time points after intravenous injection of nude mice with WT, NatD-KO, or NatD-KO + FOXA2 MDA-MB-231-luc cells from day 1 (D1) to day 45 (D45).

(F) Normalized BLI signals of lung tumors of corresponding mice recorded at the indicated time points. Two-way ANOVA test, $n = 5$, $**p < 0.01$. Data are represented as mean \pm SD.

(G) (left panels) Representative images showing luciferase activity in lungs from nude mice acquired 45 days after intravenous injection with WT, NatD-KO, or NatD-KO + FOXA2 MDA-MB-231-luc cells. (right panels) Quantification of total lung bioluminescence from nude mice in the WT, NatD-KO, and NatD-KO + FOXA2 groups. One-way ANOVA test, $n = 5$, $**p < 0.01$. Data are represented as mean \pm SD.

(H) Representative images of H&E- and IHC-stained histological sections of lungs from nude mice injected with WT, NatD-KO, or NatD-KO + FOXA2 MDA-MB-231-luc cells. Scale bar, 10 μ m.

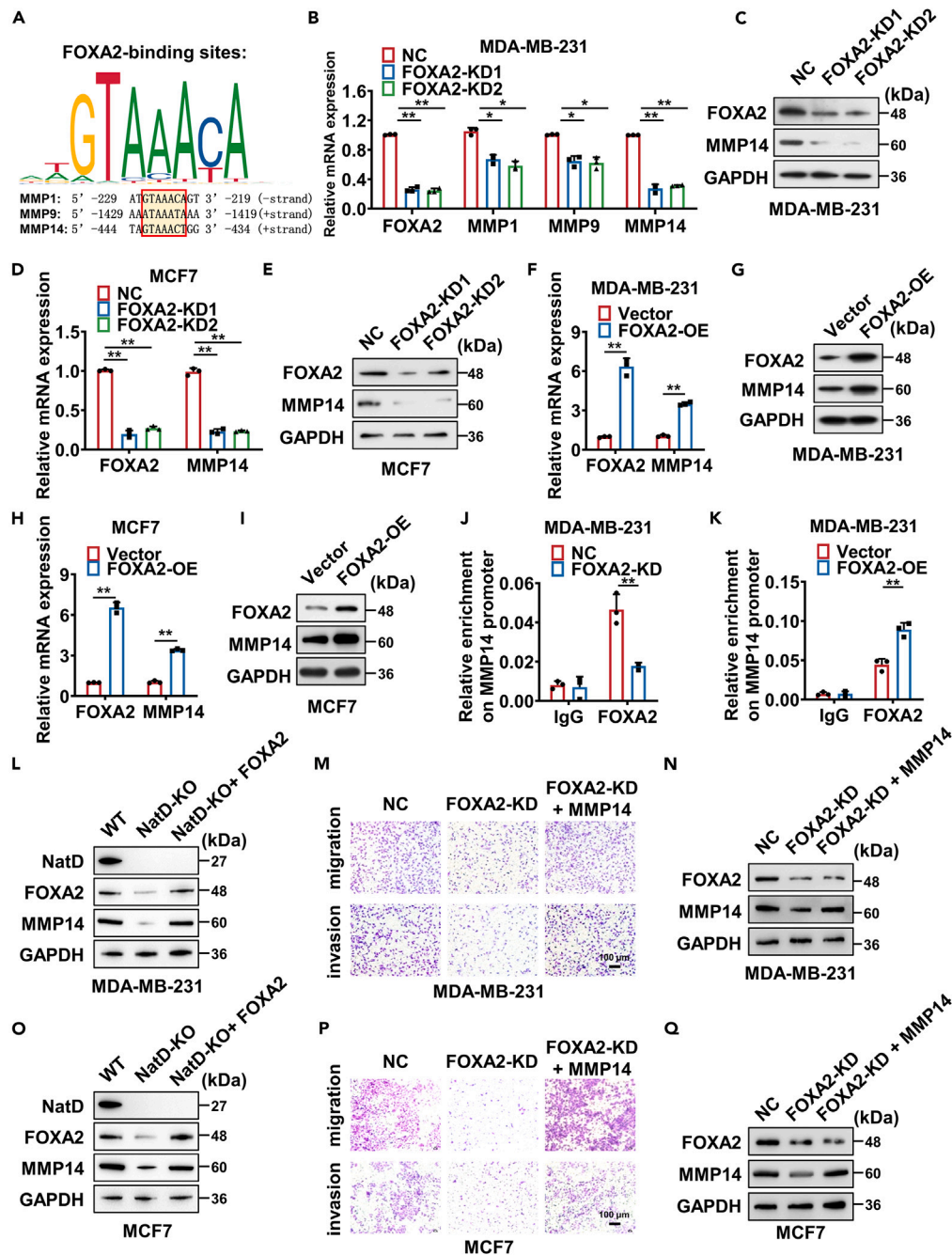


Figure 5. MMP14 is a direct downstream target of FOXA2 in breast cancer cells

(A) (top) FOXA2 consensus binding site from the JASPAR database. (bottom) The JASPAR online tools predicted the possible FOXA2-binding motifs on the promoter region of MMP1, MMP9, and MMP14.

(B) The mRNA expression of MMPs (including MMP1, MMP9, and MMP14) in MDA-MB-231 cells transfected with the scrambled negative control (NC) or FOXA2-specific siRNAs (FOXA2-KD) was measured by qRT-PCR. One-way ANOVA test, $n = 3$, $*p < 0.05$, $**p < 0.01$ vs. indicated control. Data are represented as mean \pm SD.

(C) The protein expression of FOXA2 and MMP14 was detected by western blot analysis in NC and FOXA2-KD MDA-MB-231 cells.

(D and E) The mRNA (D) and protein (E) expression of FOXA2 and MMP14 in NC and FOXA2-KD MCF7 cells was measured by qRT-PCR and western blot analysis. One-way ANOVA test, $n = 3$, $**p < 0.01$ vs. indicated control. Data are represented as mean \pm SD.

(F and G) The mRNA (F) and protein (G) expression of FOXA2 and MMP14 in MDA-MB-231 cells transfected with vector or FOXA2 expression plasmid were measured by qRT-PCR and western blot analysis. Student's t test, $n = 3$, $**p < 0.01$ vs. indicated control. Data are represented as mean \pm SD.

Figure 5. Continued

(H and I) The mRNA (H) and protein (I) expression of FOXA2 and MMP14 in MCF7 cells transfected with vector and FOXA2 expression plasmid were measured by qRT-PCR and western blot analysis. Student's *t* test, $n = 3$, $**p < 0.01$ vs. indicated control. Data are represented as mean \pm SD.
 (J) ChIP analysis of FOXA2 binding to the promoter of MMP14 in MDA-MB-231 cells transfected with NC and FOXA2-specific siRNAs. Student's *t* test, $n = 3$, $**p < 0.01$ vs. indicated control. Data are represented as mean \pm SD.
 (K) ChIP analysis of FOXA2 binding to the promoter of MMP14 in MDA-MB-231 cells transfected with vector or FOXA2 expression plasmid. Student's *t* test, $n = 3$, $**p < 0.01$ vs. indicated control. Data are represented as mean \pm SD.
 (L and O) Protein levels of NatD, FOXA2, and MMP14 in MDA-MB-231 (L) and MCF7 (O) cells with WT, NatD-KO, and NatD-KO + FOXA2 were detected by western blot analysis. GAPDH was used as an internal control.
 (M and P) Transwell assays of MDA-MB-231 (M) and MCF7 (P) cells with NC, FOXA2-KD, and FOXA2-KD + MMP14. Scale bar, 100 μ m.
 (N and Q) Protein levels of FOXA2 and MMP14 in MDA-MB-231 (N) and MCF7 (Q) cells with NC, FOXA2-KD, and FOXA2-KD + MMP14 were detected by western blot analysis. GAPDH was used as an internal control.

widely expressed in many cells and is overexpressed by malignant cancer cells, correlating with poor prognosis.^{53,54} For example, MMP14 plays an important role in CRC progression and prognosis and is a useful biomarker for the prediction of survival after colectomy.^{55,56} In renal cell carcinoma, circPTCH1 promotes invasion and metastasis by upregulating MMP14 expression.⁵⁷ Hu et al. reported that upregulation of MMP14 promotes cervical cancer cell adhesion and EMT, all of which contribute to cell motility and metastasis.⁵⁸ Many reports have also revealed that MMP14 plays a key role in controlling the aggressiveness of breast cancer cells.^{59,60} MMP14 overexpression also abrogates suppression of proliferation and induced apoptosis effects in breast cancer.⁶¹ In this study, we found that MMP14 is highly expressed in breast cancer, and its expression level positively correlates with FOXA2 expression and poor clinical prognosis. We provide evidence that the NatD-FOXA2 axis directly regulates MMP14 expression and hence the migration and invasion of breast cancer cells. These results further implicate MMP14 as an important driver of breast cancer metastasis.

In summary, our study shows that the NatD-FOXA2-MMP14 axis functions as a key signaling pathway to promote the migratory and invasive capabilities of breast cancer cells, providing an alternative avenue for targeted therapies for breast cancer metastasis.

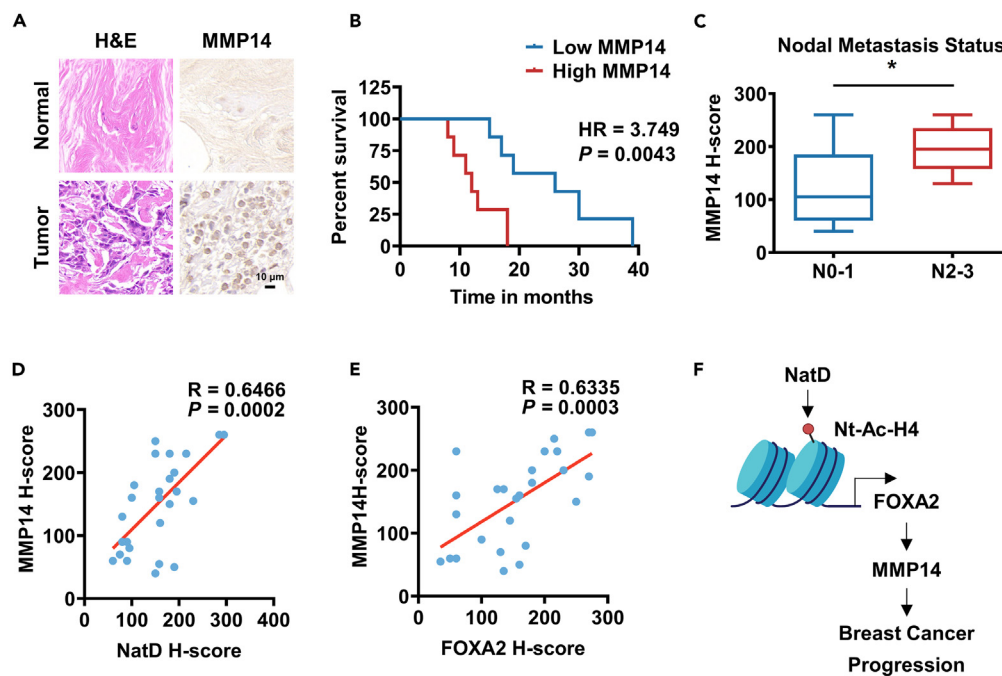


Figure 6. Upregulation of MMP14 is associated with poor prognosis in breast cancer patients

(A) Representative images of H&E staining and IHC staining of MMP14 in matched normal and breast cancer tissues. Scale bar, 10 μ m.
 (B) Kaplan-Meier plots of overall survival of patients with breast cancer stratified by MMP14 expression. Log rank test, $n = 14$, $p = 0.0043$, HR = 3.749.
 (C) Correlation of MMP14 expression with lymph node metastasis in breast cancer patients. Student's *t* test, $n(N0-1) = 18$, $n(N2-3) = 10$, $*p < 0.05$. Data are represented as mean \pm SD.
 (D) The correlation analysis of NatD and MMP14 levels in breast cancer tissues. Pearson correlation, $n = 28$, $R = 0.6466$, $p = 0.0002$.
 (E) The correlation analysis of FOXA2 and MMP14 levels in breast cancer tissues. Pearson correlation, $n = 28$, $R = 0.6335$, $p = 0.0003$.
 (F) A schematic diagram illustrating that NatD acetylates histone H4 (Nt-Ac-H4) on the promoter to promote the expression of the transcription factor FOXA2, thereby activating MMP14 gene expression and facilitating breast cancer metastasis.

Limitations of the study

In this study, we show that the NatD-FOXA2-MMP14 axis functions as a key signaling pathway to promote the migratory and invasive capabilities of breast cancer cells. Depletion of NatD directly represses the expression of a transcription factor, forkhead box A2 (FOXA2), and is accompanied by a significant reduction in Nt-Ac-H4 enrichment at the FOXA2 promoter. Furthermore, we show that FOXA2 promotes the migration and invasion of breast cancer cells by activating the expression of MMP14. However, our *in vivo* study only demonstrated that knockout of NatD inhibits lung metastasis in triple-negative breast cancer. The exact role of NatD *in vivo* needs to be further explored. Moreover, there might be other downstream target genes of NatD in addition to FOXA2 and MMP14. Therefore, further studies will consolidate our conclusions.

STAR★METHODS

Detailed methods are provided in the online version of this paper and include the following:

- KEY RESOURCES TABLE
- RESOURCE AVAILABILITY
 - Lead contact
 - Materials availability
 - Data and code availability
- EXPERIMENTAL MODEL AND STUDY PARTICIPANT DETAILS
 - Ethics approval and consent to participate
 - Clinical samples
 - Animal studies
 - Consent for publication
- METHOD DETAILS
 - Cell culture
 - LentiCRISPR, and siRNA interference assay
 - Immunohistochemical (IHC) staining
 - Protein extraction and western blot analysis
 - Transwell assay
 - RNA isolation and quantitative real-time PCR (qRT-PCR)
 - Chromatin immunoprecipitation (ChIP)
 - Gene set enrichment analysis (GSEA) and gene ontology (GO) analysis
 - Bioinformatics analysis
- QUANTIFICATION AND STATISTICAL ANALYSIS

SUPPLEMENTAL INFORMATION

Supplemental information can be found online at <https://doi.org/10.1016/j.isci.2024.108840>.

ACKNOWLEDGMENTS

We are grateful to all members of the Zhao, Su, and Wei laboratories for valuable discussions. This work was supported by National Natural Science Foundation of China (grant numbers: 31970615 and 32270619) and Nanjing Municipal Commission of Science and Technology (grant numbers: 201911006).

AUTHOR CONTRIBUTIONS

Conceptualization, J.W., L.S., and Q.Z.; investigation, M.X., B.Y., P.L., Q.L., and D.W.; data curation, M.X. and B.Y.; formal analysis, M.X.; bioinformatics analysis, J.X.; methodology, P.L., Q.L., and D.W.; pathological analysis, B.C. and L.S.; supervision, J.W., L.S., and Q.Z.

DECLARATION OF INTERESTS

The authors declare no competing interests.

Received: August 25, 2023

Revised: December 9, 2023

Accepted: January 3, 2024

Published: January 9, 2024

REFERENCES

1. Arnesen, T., Van Damme, P., Polevoda, B., Helsen, K., Evjenth, R., Colaert, N., Varhaug, J.E., Vandekerckhove, J., Lillehaug, J.R., Sherman, F., and Gevaert, K. (2009). Proteomics analyses reveal the evolutionary conservation and divergence of N-terminal acetyltransferases from yeast and humans. *Proc. Natl. Acad. Sci. USA* *106*, 8157–8162.
2. Hwang, C.S., Shemorry, A., and Varshavsky, A. (2010). N-terminal acetylation of cellular proteins creates specific degradation signals. *Science* *327*, 973–977.
3. Forte, G.M.A., Pool, M.R., and Stirling, C.J. (2011). N-terminal acetylation inhibits protein targeting to the endoplasmic reticulum. *PLoS Biol.* *9*, e1001073.
4. Behnia, R., Panic, B., Whyte, J.R.C., and Munro, S. (2004). Targeting of the Arf-like GTPase Arl3p to the Golgi requires N-terminal acetylation and the membrane protein Sys1p. *Nat. Cell Biol.* *6*, 405–413.
5. Aksnes, H., Ree, R., and Arnesen, T. (2019). Co-translational, Post-translational, and Non-catalytic Roles of N-Terminal Acetyltransferases. *Mol. Cell* *73*, 1097–1114.
6. Arnesen, T. (2011). Towards a functional understanding of protein N-terminal acetylation. *PLoS Biol.* *9*, e1001074.
7. Magin, R.S., Liszczak, G.P., and Marmorstein, R. (2015). The molecular basis for histone H4- and H2A-specific amino-terminal acetylation by NatD. *Structure* *23*, 332–341.
8. Mullen, J.R., Kayne, P.S., Moerschell, R.P., Tsunasawa, S., Gribskov, M., Colavito-Shepanski, M., Grunstein, M., Sherman, F., and Sternglanz, R. (1989). Identification and characterization of genes and mutants for an N-terminal acetyltransferase from yeast. *EMBO J.* *8*, 2067–2075.
9. Ju, J., Chen, A., Deng, Y., Liu, M., Wang, Y., Wang, Y., Nie, M., Wang, C., Ding, H., Yao, B., et al. (2017). NatD promotes lung cancer progression by preventing histone H4 serine phosphorylation to activate Slug expression. *Nat. Commun.* *8*, 928.
10. Demetriadou, C., Pavlou, D., Mpekris, F., Achilleos, C., Stylianopoulos, T., Zaravinos, A., Papageorgis, P., and Kirmizis, A. (2019). NAA40 contributes to colorectal cancer growth by controlling PRMT5 expression. *Cell Death Dis.* *10*, 236.
11. Demetriadou, C., Koufaris, C., and Kirmizis, A. (2020). Histone N-alpha terminal modifications: genome regulation at the tip of the tail. *Epigenet. Chromatin* *13*, 29.
12. Liu, Z., Liu, Y., Wang, H., Ge, X., Jin, Q., Ding, G., Hu, Y., Zhou, B., Chen, Z., Ge, X., et al. (2009). Patt1, a novel protein acetyltransferase that is highly expressed in liver and downregulated in hepatocellular carcinoma, enhances apoptosis of hepatoma cells. *Int. J. Biochem. Cell Biol.* *41*, 2528–2537.
13. Pavlou, D., and Kirmizis, A. (2016). Depletion of histone N-terminal-acetyltransferase Naa40 induces p53-independent apoptosis in colorectal cancer cells via the mitochondrial pathway. *Apoptosis* *21*, 298–311.
14. Camolotto, S.A., Pattabiraman, S., Mosbrugger, T.L., Jones, A., Belova, V.K., Orstad, G., Streiff, M., Salmond, L., Stubben, C., Kaestner, K.H., and Snyder, E.L. (2018). FoxA1 and FoxA2 drive gastric differentiation and suppress squamous identity in NKX2-1-negative lung cancer. *Elife* *7*, e38579.
15. Iwafuchi-Doi, M., and Zaret, K.S. (2014). Pioneer transcription factors in cell reprogramming. *Gene Dev.* *28*, 2679–2692.
16. Liu, Y., Chen, T., Guo, M., Li, Y., Zhang, Q., Tan, G., Yu, L., and Tan, Y. (2021). FOXA2-Interacting FOXP2 Prevents Epithelial-Mesenchymal Transition of Breast Cancer Cells by Stimulating E-Cadherin and PHF2 Transcription. *Front. Oncol.* *11*, 605025.
17. Friedman, J.R., and Kaestner, K.H. (2006). The Foxa family of transcription factors in development and metabolism. *Cell. Mol. Life Sci.* *63*, 2317–2328.
18. Li, Z., Tuteja, G., Schug, J., and Kaestner, K.H. (2012). Foxa1 and Foxa2 are essential for sexual dimorphism in liver cancer. *Cell* *148*, 72–83.
19. Tang, Y., Shu, G., Yuan, X., Jing, N., and Song, J. (2011). FOXA2 functions as a suppressor of tumor metastasis by inhibition of epithelial-to-mesenchymal transition in human lung cancers. *Cell Res.* *21*, 316–326.
20. Genga, R.M.J., Kernfeld, E.M., Parsi, K.M., Parsons, T.J., Ziller, M.J., and Maehr, R. (2019). Single-Cell RNA-Sequencing-Based CRISPRi Screening Resolves Molecular Drivers of Early Human Endoderm Development. *Cell Rep.* *27*, 708–718.e10.
21. Wang, B., Liu, G., Ding, L., Zhao, J., and Lu, Y. (2018). FOXA2 promotes the proliferation, migration and invasion, and epithelial mesenchymal transition in colon cancer. *Exp. Ther. Med.* *16*, 133–140.
22. Zhao, J.Y., Hu, Y.W., Li, S.F., Hu, Y.R., Ma, X., Wu, S.G., Wang, Y.C., Gao, J.J., Sha, Y.H., Zheng, L., and Wang, Q. (2014). Dihydrocapsaicin down-regulates apoM expression through inhibiting Foxa2 expression and enhancing LXRalpha expression in HepG2 cells. *Lipids Health Dis.* *13*, 50.
23. Salem, M., O'Brien, J.A., Bernaudo, S., Shaver, H., Ye, G., Brkić, J., Amleh, A., Vanderhyden, B.C., Refky, B., Yang, B.B., et al. (2018). miR-590-3p Promotes Ovarian Cancer Growth and Metastasis via a Novel FOXA2-Versican Pathway. *Cancer Res.* *78*, 4175–4190.
24. Niland, S., Riscanevo, A.X., and Eble, J.A. (2021). Matrix Metalloproteinases Shape the Tumor Microenvironment in Cancer Progression. *Int. J. Mol. Sci.* *23*, 146.
25. Alexander, S.M., Jackson, K.J., Bushnell, K.M., and McGuire, P.G. (1997). Spatial and temporal expression of the 72-kDa type IV collagenase (MMP-8) correlates with development and differentiation of valves in the embryonic avian heart. *Dev. Dynam.* *209*, 261–268.
26. Belhocine, M., Gernigon-Spychalowicz, T., Benazzoug, Y., and Exbrayat, J.M. (2012). Gelatinase B (MMP-9) immunorexpression in the Libyan jird (*Meriones libycus*) coagulating gland during seasonal cycle of reproduction and after castration. *Fund. Clin. Pharmacol.* *26*, 9.
27. Chen, Z., Wang, H., Xia, Y., Yan, F., and Lu, Y. (2018). Therapeutic Potential of Mesenchymal Cell-Derived miRNA-150-5p-Expressing Exosomes in Rheumatoid Arthritis Mediated by the Modulation of MMP14 and VEGF. *J. Immunol.* *201*, 2472–2482.
28. Han, K.Y., Dugas-Ford, J., Seiki, M., Chang, J.H., and Azar, D.T. (2015). Evidence for the Involvement of MMP14 in MMP2 Processing and Recruitment in Exosomes of Corneal Fibroblasts. *Invest Ophth Vis Sci* *56*, 5323–5329.
29. Lu, H., Hong, J., Peng, D., Bhat, A.A., Chen, Z., Zaika, A., and El-Rifai, W.M. (2017). A New Function of Ape1 in Barrett's Esophagus and Esophageal Adenocarcinoma: Ape1 Upregulates Mmp2 and Mmp14 to Promote Invasion. *Gastroenterology* *152*, S237.
30. Teng, S., Li, Y.E., Yang, M., Qi, R., Huang, Y., Wang, Q., Zhang, Y., Chen, S., Li, S., Lin, K., et al. (2020). Tissue-specific transcription reprogramming promotes liver metastasis of colorectal cancer. *Cell Res.* *30*, 34–49.
31. Scheibner, K., Schirge, S., Burtscher, I., Büttner, M., Sterr, M., Yang, D., Böttcher, A., Ansarullah, Imler, M., Imler, M., Beckers, J., et al. (2021). Epithelial cell plasticity drives endoderm formation during gastrulation. *Nat. Cell Biol.* *23*, 692–703.
32. Chen, Z., Xiao, Q., Shen, Y., and Xue, C. (2022). FOXA2 promotes esophageal cancer migration and metastasis by activating CXCR4 expression. *Biochem. Biophys. Res. Commun.* *625*, 16–22.
33. Linder, S. (2007). The matrix corroded: podosomes and invadopodia in extracellular matrix degradation. *Trends Cell Biol.* *17*, 107–117.
34. Sato, H., and Seiki, M. (1996). Membrane-type matrix metalloproteinases (MT-MMPs) in tumor metastasis. *J. Biochem.* *119*, 209–215.
35. Naba, A., Clauser, K.R., Hoersch, S., Liu, H., Carr, S.A., and Hynes, R.O. (2012). The matrisome: in silico definition and in vivo characterization by proteomics of normal and tumor extracellular matrices. *Mol. Cell. Proteomics* *11*, M111.014647.
36. Wang, J., Zhu, C.P., Hu, P.F., Qian, H., Ning, B.F., Zhang, Q., Chen, F., Liu, J., Shi, B., Zhang, X., and Xie, W.F. (2014). FOXA2 suppresses the metastasis of hepatocellular carcinoma partially through matrix metalloproteinase-9 inhibition. *Carcinogenesis* *35*, 2576–2583.
37. Lappalainen, U., Whitsett, J.A., Wert, S.E., Tichelaar, J.W., and Bry, K. (2005). Interleukin-1beta causes pulmonary inflammation, emphysema, and airway remodeling in the adult murine lung. *Am. J. Respir. Cell Mol. Biol.* *32*, 311–318.
38. Starheim, K.K., Gevaert, K., and Arnesen, T. (2012). Protein N-terminal acetyltransferases: when the start matters. *Trends Biochem. Sci.* *37*, 152–161.
39. Koufaris, C., and Kirmizis, A. (2021). Identification of NAA40 as a Potential Prognostic Marker for Aggressive Liver Cancer Subtypes. *Front. Oncol.* *11*, 691950.
40. Demetriadou, C., Raoukka, A., Charidemou, E., Mylonas, C., Michael, C., Parekh, S., Koufaris, C., Skourides, P., Papageorgis, P., Tessarz, P., and Kirmizis, A. (2022). Histone N-terminal acetyltransferase NAA40 links one-carbon metabolism to chemoresistance. *Oncogene* *41*, 571–585.
41. Koufaris, C., and Kirmizis, A. (2020). N-Terminal Acetyltransferases Are Cancer-Essential Genes Prevalently Upregulated in Tumours. *Cancers* *12*, 2631.
42. Deng, Y., Deng, S., Ho, Y.H., Gardner, S.M., Huang, Z., Marmorstein, R., and Huang, R. (2021). Novel Bisubstrate Inhibitors for Protein N-Terminal Acetyltransferase D. *J. Med. Chem.* *64*, 8263–8271.
43. Ho, Y.H., Chen, L., and Huang, R. (2021). Development of A Continuous Fluorescence-Based Assay for N-Terminal Acetyltransferase D. *Int. J. Mol. Sci.* *22*, 594.

44. Tu, M.J., Pan, Y.Z., Qiu, J.X., Kim, E.J., and Yu, A.M. (2016). MicroRNA-1291 targets the FOXA2-AGR2 pathway to suppress pancreatic cancer cell proliferation and tumorigenesis. *Oncotarget* *7*, 45547–45561.
45. Vorvis, C., Hatzia Apostolou, M., Mahurkar-Joshi, S., Koutsoumpa, M., Williams, J., Donahue, T.R., Poultsides, G.A., Eibl, G., and Iliopoulos, D. (2016). Transcriptomic and CRISPR/Cas9 technologies reveal FOXA2 as a tumor suppressor gene in pancreatic cancer. *Am. J. Physiol. Gastrointest. Liver Physiol.* *310*, G1124–G1137.
46. Bow, Y.D., Wang, Y.Y., Chen, Y.K., Su, C.W., Hsu, C.W., Xiao, L.Y., Yuan, S.S., and Li, R.N. (2020). Silencing of FOXA2 decreases E-cadherin expression and is associated with lymph node metastasis in oral cancer. *Oral Dis.* *26*, 756–765.
47. Tarone, G., Cirillo, D., Giancotti, F.G., Comoglio, P.M., and Marchisio, P.C. (1985). Rous-Sarcoma Virus-Transformed Fibroblasts Adhere Primarily at Discrete Protrusions of the Ventral Membrane Called Podosomes. *Exp. Cell Res.* *159*, 141–157.
48. Chen, W.T. (1989). Proteolytic Activity of Specialized Surface Protrusions Formed at Rosette Contact Sites of Transformed-Cells. *J. Exp. Zool.* *251*, 167–185.
49. Lehti, K., Allen, E., Birkedal-Hansen, H., Holmbeck, K., Miyake, Y., Chun, T.H., and Weiss, S.J. (2005). An MT1-MMP-PDGF receptor-beta axis regulates mural cell investment of the microvasculature. *Gene Dev.* *19*, 979–991.
50. Zhou, Z., Apte, S.S., Soininen, R., Cao, R., Baaklini, G.Y., Rauser, R.W., Wang, J., Cao, Y., and Tryggvason, K. (2000). Impaired endochondral ossification and angiogenesis in mice deficient in membrane-type matrix metalloproteinase I. *Proc. Natl. Acad. Sci. USA* *97*, 4052–4057.
51. Gutiérrez-Fernández, A., Soria-Valles, C., Osorio, F.G., Gutiérrez-Abril, J., Garabaya, C., Aguirre, A., Fueyo, A., Fernández-García, M.S., Puente, X.S., and López-Otín, C. (2015). Loss of MT1-MMP causes cell senescence and nuclear defects which can be reversed by retinoic acid. *EMBO J.* *34*, 1875–1888.
52. Niewiarowska, J., Brézillon, S., Sacewicz-Hofman, I., Bednarek, R., Maquart, F.X., Malinowski, M., Wiktorska, M., Wegrowski, Y., and Cierniewski, C.S. (2011). Lumican inhibits angiogenesis by interfering with alpha 2 beta 1 receptor activity and downregulating MMP-14 expression. *Thromb. Res.* *128*, 452–457.
53. Gifford, V., and Itoh, Y. (2019). MT1-MMP-dependent cell migration: proteolytic and non-proteolytic mechanisms. *Biochem. Soc. Trans.* *47*, 811–826.
54. Dong, Y., Chen, G., Gao, M., and Tian, X. (2015). Increased expression of MMP14 correlates with the poor prognosis of Chinese patients with gastric cancer. *Gene* *563*, 29–34.
55. Cui, G., Cai, F., Ding, Z., and Gao, L. (2019). MMP14 predicts a poor prognosis in patients with colorectal cancer. *Hum. Pathol.* *83*, 36–42.
56. Hu, X.T., Xing, W., Zhao, R.S., Tan, Y., Wu, X.F., Ao, L.Q., Li, Z., Yao, M.W., Yuan, M., Guo, W., et al. (2020). HDAC2 inhibits EMT-mediated cancer metastasis by downregulating the long noncoding RNA H19 in colorectal cancer. *J. Exp. Clin. Oncol. Res.* *39*, 270.
57. Liu, H., Hu, G., Wang, Z., Liu, Q., Zhang, J., Chen, Y., Huang, Y., Xue, W., Xu, Y., and Zhai, W. (2020). circPTCH1 promotes invasion and metastasis in renal cell carcinoma via regulating miR-485-5p/MMP14 axis. *Theranostics* *10*, 10791–10807.
58. Hu, Y., Wu, F., Liu, Y., Zhao, Q., and Tang, H. (2019). DNMT1 recruited by EZH2-mediated silencing of miR-484 contributes to the malignancy of cervical cancer cells through MMP14 and HNF1A. *Clin. Epigenetics* *11*, 186.
59. Jiang, W.G., Davies, G., Martin, T.A., Parr, C., Watkins, G., Mason, M.D., and Mansel, R.E. (2006). Expression of membrane type-1 matrix metalloproteinase, MT1-MMP in human breast cancer and its impact on invasiveness of breast cancer cells. *Int. J. Mol. Med.* *17*, 583–590.
60. Mylona, E., Nomikos, A., Magkou, C., Kamberou, M., Papassideri, I., Keramopoulos, A., and Nakopoulou, L. (2007). The clinicopathological and prognostic significance of membrane type 1 matrix metalloproteinase (MT1-MMP) and MMP-9 according to their localization in invasive breast carcinoma. *Histopathology* *50*, 338–347.
61. Saby, C., Rammal, H., Magnien, K., Buache, E., Brassart-Pasco, S., Van-Gulick, L., Jeannesson, P., Maquoi, E., and Morjani, H. (2018). Age-related modifications of type I collagen impair DDR1-induced apoptosis in non-invasive breast carcinoma cells. *Cell Adh. Migr.* *12*, 335–347.

STAR★METHODS

KEY RESOURCES TABLE

REAGENT or RESOURCE	SOURCE	IDENTIFIER
Antibodies		
Anti-NatD	Genscript	Cat# A311140394
Anti-Nt-Ac-H4	Genscript	Cat# A312010093
Anti-FOXA2	Proteintech	Cat# 22474-1-AP; RRID: AB_2879110
Anti-MMP14	Millipore	Cat# AB8345; RRID: AB_92348
Anti-GAPDH	Proteintech	Cat# 60004-1-IG; RRID: AB_2107436
Bacterial and virus strains		
lentiCRISPR v2 vector	Addgene	Cat# 52961
Biological samples		
breast cancer and adjacent normal tissue sections	Nanjing Drum Tower Hospital	N/A
Chemicals, peptides, and recombinant proteins		
Matrigel	BD	Cat# 356234
RNAiso plus	TAKARA	Cat# 9109
HiScript Q RT SuperMix for qPCR	Vazyme	Cat# R123
qPCR SYBR Green Master Mix	Vazyme	Cat# Q121
D-Luciferin Potassium Salt	Yeasen	Cat# 40902
Critical commercial assays		
Chromatin IP Kit	Cell Signaling Technology	Cat# 9004
Deposited data		
RNA-seq data	GEO database	GSE230625
Experimental models: Cell lines		
MDA-MB-231	Shanghai Institute of Cell Biology	SCSP-5043
MCF7	Shanghai Institute of Cell Biology	SCSP-531
HEK293T	Shanghai Institute of Cell Biology	GNHu17
Experimental models: Organisms/strains		
BALB/c-nu mice	the Animal Core Facility of Nanjing Medical University	N/A
Oligonucleotides		
NatD-sgRNA1: ATTGAATGTAAGCGAGTGTC	This paper	N/A
NatD-sgRNA2: CATGGTTTGCATATTCGTTT	This paper	N/A
FOXA2-siRNA1: AAAUGGACCUCAAGGCCUA	This paper	N/A
FOXA2-siRNA2: GAACACCACUACGCCUUA	This paper	N/A
NatD-F: ATGTAAGCGAGTGTCTGGACT	This paper	N/A
NatD-R: TGGTTTGCATATTCGTTTTGGTC	This paper	N/A
FOXA2-F: CCCACAAAATGGACCTCAAG	This paper	N/A
FOXA2-R: GAGTACACCCCTGGTAGTAG	This paper	N/A
GAPDH-F: GGAGCGAGATCCCTCCAAAAT	This paper	N/A
GAPDH-R: GGCTGTTGTCATACTTCTCATGG	This paper	N/A
MMP14-F: GGCTACAGCAATATGGCTACC	This paper	N/A
MMP14-R: GATGGCCGCTGAGAGTGAC	This paper	N/A
CXCR4-F: ACTACACCGAGGAAATGGGCT	This paper	N/A

(Continued on next page)

Continued

REAGENT or RESOURCE	SOURCE	IDENTIFIER
CXCR4-R: CCCACAATGCCAGTTAAGAAGA	This paper	N/A
ITGB2-F: AAGTGACGCTTTACCTGCGAC	This paper	N/A
ITGB2-R: AAGCATGGAGTAGGAGAGGTC	This paper	N/A
ITGB3-F: CATGAAGGATGATCTGTGGAGC	This paper	N/A
ITGB3-R: AATCCGCAGTTACTGGTGAG	This paper	N/A
MMP1-F: AAAATTACACGCCAGATTTGCC	This paper	N/A
MMP1-R: GGTGTGACACTACTCCAGAGTTG	This paper	N/A
MMP9-F: AGACCTGGGCAGATTCCAAAC	This paper	N/A
MMP9-R: CGGCAAGTCTTCCGAGTAGT	This paper	N/A
E-cadherin-F: ATTTTCCCTCGACACCCGAT	This paper	N/A
E-cadherin-R: TCCCAGGCGTAGACCAAGA	This paper	N/A
ADAMTS1-F: ACTGGAAGCATAAGAAAGAAGCG	This paper	N/A
ADAMTS1-R: AATTCTGCCATCGACTGGTCT	This paper	N/A
CD44-F: CTGCCGCTTTGCAGGTGTA	This paper	N/A
CD44-R: CATTGTGGCAAGGTGCTATT	This paper	N/A
ChIP-FOXA2-F1: GCACACCTCCACGTTCACTA	This paper	N/A
ChIP-FOXA2-R1: TAATAAGCCCGCCGAGTGAG	This paper	N/A
ChIP-MMP14-F1: TGCACCACAAAAGGCAACTTAG	This paper	N/A
ChIP-MMP14-R1: CCCAGTGCCTCCTTTCC	This paper	N/A
ChIP-MMP14-F2: GGATTTTTTAGCAGCAGAGGGAG	This paper	N/A
ChIP-MMP14-R2: CTCAGAGTGTGGATGGTGG	This paper	N/A
ChIP-MMP14-F3: CTGTGGGGTAGGTAGCTGTT	This paper	N/A
ChIP-MMP14-R3: ATGAAAACAAAGGTCTTTTGCCTT	This paper	N/A
ChIP-MMP14-F4: CAGTTTTGGCCAGGCAGT	This paper	N/A
ChIP-MMP14-R4: CTGACACCAGATGCTTGC	This paper	N/A
ChIP-MMP14-F5: TGTAATCCCAGCACTTTGGG	This paper	N/A
ChIP-MMP14-R5: CTCCCGAGTTTAAGCGATTC	This paper	N/A

Recombinant DNA

pcDNA3.1-NatD	This paper	N/A
pcDNA3.1-FOXA2	This paper	N/A
pcDNA3.1-MMP14	This paper	N/A

Software and algorithms

ImageJ	National Institutes of Health	V1.53e
Graphpad Prism	GraphPad	V8.0
GSEA software	Broad Institute	V4.3.2
Metascape	Metascape	V3.5

RESOURCE AVAILABILITY

Lead contact

Further information and requests for resources and reagents should be directed to and will be fulfilled by the lead contact, Quan Zhao (qzhao@nju.edu.cn).

Materials availability

This study did not generate new unique reagents.

Data and code availability

- The RNA-seq data have been deposited at GEO and are publicly available as of the date of publication (GSE230625).
- This paper does not report original code.
- Any additional information required to reanalyze the data reported in this paper is available from the [lead contact](#) upon request.

EXPERIMENTAL MODEL AND STUDY PARTICIPANT DETAILS

Ethics approval and consent to participate

All the authors consented to participate in this study. This research was approved by the Ethics Committee of the Affiliated Drum Tower Hospital, Medical School of Nanjing University (IRB Report ID: 2020-134-01) and was conducted in compliance with the tenets of the Declaration of Helsinki. All the animal experiments were approved by the Institutional Animal Care and Use Committee (IACUC) of Nanjing Medical University (IACUC-2011053).

Clinical samples

A total of 132 pairs of breast cancer and adjacent normal tissue sections were obtained from Nanjing Drum Tower Hospital (IRB Report ID: 2020-134-01). All patients provided written informed consent for participation in this study. The study on fresh clinical samples was approved by the ethics committee of Nanjing Drum Tower Hospital. The clinical data of all breast cancer patients are displayed in [Tables S1](#) and [S2](#). All the patients involved were women. There were no restrictions on race or ethnicity, but all patients who were included were Chinese.

This Tumor, Nodes, Metastasis (TNM) system was modeled after the American Joint Committee on Cancer (AJCC) TNM staging system for breast cancer (www.cancerstaging.org). There are five stages of breast cancer designated 0, I, II, III, IV. The higher the number, the greater the cancer has spread. The cancer is staged when patients are first diagnosed. None of the patients enrolled in these studies were graded stage IV.

Animal studies

A group of 4-week-old female BALB/c nude mice were purchased from the Animal Core Facility of Nanjing Medical University. Cell line-derived xenograft (CDX) mouse models were used in this study. The number of animals used for each experiment is indicated in each figure or figure legend. Prior to carrying out the experiment, mice were randomly assigned to different treatment groups. 1×10^5 MDA-MB-231-luc cells (MDA-MB-231 cells labeled with luciferase tag) were suspended in 100 μ l PBS and injected into nude mice through the caudal vein. Thereafter, luciferase signals in the mice were measured every 2 weeks. For imaging, the mice were injected intraperitoneally with D-Luciferin Potassium Salt (Yeasen, Shanghai, China) at 150 mg/kg of body weight and imaged in the IVIS system (PerkinElmer, USA) after 10 min while anesthetized. On the 45th day of the experiment, the mice were sacrificed and subsequently dissected. Their lungs were collected for observation *in vitro* and fixed with 4% paraformaldehyde for subsequent experiments, such as hematoxylin-eosin (HE) and IHC staining. A blinding strategy when assessing the outcome was used whenever possible.

Consent for publication

Written informed consent for publication was obtained from all the participants.

METHOD DETAILS

Cell culture

MDA-MB-231, MCF7, and HEK293T cells were purchased from the Shanghai Institute of Cell Biology, Chinese Academy of Sciences (Shanghai, China). Cells were cultured at 37°C in a humidified air atmosphere containing 5% carbon dioxide in DMEM with 10% fetal bovine serum (FBS) (ExCell Bio, Uruguay). Human cancer cell lines were recently authenticated by Genetic Testing Biotechnology Corporation (Suzhou, China) using short tandem repeat (STR) profiling. No cell line used in this paper is listed in the database of commonly misidentified cell lines maintained by the International Cell Line Authentication Committee (ICLAC). All lines were found to be negative for mycoplasma contamination.

LentiCRISPR, and siRNA interference assay

For human NatD targeting, CRISPR target sequences were cloned into the lentiCRISPR v2 vector (Addgene, Cat# 52961). The sgDNA target sequences of NatD were inserted into the lentiCRISPR v2 lentiviral vector according to the manufacturer's recommendations. The oligonucleotide sequences for human NatD sgDNA in this study are listed in [key resources table](#). Lentivirus production in HEK293T cells and infection of MDA-MB-231 and MCF7 cells were performed in accordance with standard protocols. Transduced cells were selected by puromycin. siRNA against FOXA2 and scrambled negative control (NC) siRNA were synthesized by Tsingke Co. Ltd. (China) and are listed in [key resources table](#).

Immunohistochemical (IHC) staining

IHC staining was performed using paraffin-embedded sections of biopsies from breast cancer patients and controls according to standard protocols. Slides were briefly incubated with primary antibodies (anti-NatD, 1:100; Genscript, Nanjing, China), followed by incubation with horseradish peroxidase-conjugated goat anti-rabbit secondary antibody. Antibody binding was visualized using a 2-Solution DAB Kit. Finally, NatD expression was evaluated by two experienced pathologists working independently without reference to the clinical data. The intensity of immunostaining was documented as being 0–3: 0, negative; 1, weak; 2, moderate; and 3, strong. The H-score was calculated by adding the multiplication product of the different staining intensities (0–3) to the percentage of positive cells, i.e., H-score (0–300 scale) = $3 \times (\% \text{ at } 3+) + 2 \times (\% \text{ at } 2+) + 1 \times (\% \text{ at } 1+)$. For survival analyses, patient overall survival was stratified by expression of the gene of interest between two groups: high (\geq median value) and low ($<$ median value), and was presented as Kaplan-Meier plots and tested for significance using log-rank tests.

Protein extraction and western blot analysis

MDA-MB-231 and MCF7 cells were extracted by RIPA lysis buffers (50mM Tris, 150mM NaCl, 1% NP-40, 0.5% sodium deoxycholate, 0.1% SDS) containing protease inhibitors. Samples containing equal amounts of protein were separated by SDS-PAGE. After electrophoresis, the proteins were transferred to a PVDF membrane (Millipore, Billerica, MA, USA) and blocked with 5% skim milk at room temperature for 2 h. The membranes were incubated overnight at 4°C with the following primary antibodies: anti-NatD (1:1000; Genscript), anti-Nt-Ac-H4 (1:1000; Genscript), anti-FOXA2 (1:1000; Proteintech, Wuhan, China), anti-MMP14 (1:1000; Millipore), and anti-GAPDH (1:50000; Proteintech). After being washed with $1 \times$ TBST 3 times, the membranes were incubated with horseradish peroxidase (HRP)-conjugated Affinipure Goat Anti-Rabbit IgG (H + L) (1:10,000; Proteintech) or Anti-Mouse IgG (H + L) (1:10,000; Proteintech) at room temperature for 2 hours. The proteins were visualized by chemiluminescence with ECL reagent (Tanon; Shanghai, China).

Transwell assay

Cell migration or invasion was measured using 24-well transwell chambers (aperture, 8.0 μm ; diameter, 6.5 mm; Corning, USA) in the presence or absence of Matrigel (BD Biosciences, USA) according to the manufacturer's protocol. Approximately 3×10^4 (migration assay) or 6×10^4 (invasion assay) cells in 200 μl serum-free DMEM were added to the upper compartment, and 600 μl DMEM with 10% FBS was added to the lower compartment. The transwell chambers were then incubated in a 5% CO₂ incubator at 37°C for 24 h. Cells that passed through the membrane were fixed with 100% methanol for 20 minutes, stained with 0.1% crystal violet for 30 minutes, imaged under a microscope (Nikon; Tokyo, Japan) and counted using ImageJ software.

RNA isolation and quantitative real-time PCR (qRT-PCR)

Total RNA was extracted using RNAiso plus (Takara, Japan) according to the manufacturer's protocol. RNA was converted to cDNA using HiScript Q RT SuperMix for qPCR (+gDNA wiper) (Vazyme, Nanjing, China) following the manufacturer's instructions. Gene expression was detected using AceQ qPCR SYBR Green Master Mix (Vazyme, Nanjing, China) in a 96-well plate format as described by the manufacturer's protocol. qRT-PCR primer sequences for all genes analyzed in this study are listed in [key resources table](#).

Chromatin immunoprecipitation (ChIP)

ChIP assays were performed with the SimpleChIP® Plus Enzymatic Chromatin IP Kit (Cell Signaling Technology, USA). Normal rabbit IgG served as the control. ChIP samples were analyzed by qRT-PCR. The primer sequences for ChIP are listed in [key resources table](#).

Gene set enrichment analysis (GSEA) and gene ontology (GO) analysis

Differentially expressed genes after NatD knockdown in MDA-MB-231 cells were analyzed using GSEA software (Broad Institute). GO analysis was performed using Metascape V3.5 (<https://metascape.org/>).

Bioinformatics analysis

The expression of NatD and MMP14 in breast cancer was analyzed by adopting the UALCAN website (<http://ualcan.path.uab.edu/analysis.html>). The expression of NatD in luminal, HER2 positive, triple-negative breast cancer (TNBC), and normal tissues was obtained from The Cancer Genome Atlas (TCGA) and the National Cancer Institute's Clinical Proteomic Tumor Analysis Consortium (CPTAC) databases. The datasets used and analyzed in this study are available on the Gene Expression Omnibus repository (accession number GEO: GSE12093, GSE25065, GSE9893). The NatD, FOXA2 and MMP14 overall survival curves were compared between two groups: high (\geq median value) and low ($<$ median value) expression using log-rank tests. The Relapse-free survival (RFS) analysis was performed using Kaplan-Meier curve log-rank testing, using R routine to find the best cutoff values for FOXA2 and MMP14 high- and low-expression selection.

QUANTIFICATION AND STATISTICAL ANALYSIS

Survival curves were constructed using the Kaplan-Meier method and analyzed by the log-rank test. The correlation analysis was assessed by Pearson's correlation analysis. Statistical comparisons were made through one-way ANOVA, two-way ANOVA or Student's *t* test using GraphPad Prism 8.0 Software (GraphPad Inc., La Jolla, CA, USA). The results are presented as the mean \pm SD unless otherwise indicated. The exact sample size for each experimental group is shown in every figure as the number of dots. $p < 0.05$ was considered statistically significant. * $p < 0.05$; ** $p < 0.01$; ns, not significant.